ELSEVIER

15 April 1996

OPTICS COMMUNICATIONS

Optics Communications 125 (1996) 288–301

Full length article

Synthesis of mutual intensity distributions using the fractional Fourier transform

M. Fatih Erden [a], Haldun M. Ozaktas [a], David Mendlovic [b]

[a] *Bilkent University, Electrical Engineering, 06533 Bilkent, Ankara, Turkey*

[b] *Tel-Aviv University, Faculty of Engineering, 69978 Tel-Aviv, Israel*

Received 3 August 1995; accepted 8 December 1995

Abstract

Our aim in this paper is to obtain the best synthesis of a desired mutual intensity distribution, by filtering in fractional Fourier domains. More specifically, we find the optimal fractional-domain filter that transforms a given (source) mutual intensity distribution into the desired one as closely as possible (in the minimum mean-square error sense). It is observed that, in some cases, closer approximations to the desired profile can be obtained by filtering in fractional Fourier domains, in comparison to filtering in the ordinary space or frequency domains.

Keywords: Fourier optics; Statistical optics; Fractional Fourier transforms; Mutual intensity

1. Introduction

What we know as the space and spatial frequency domains are merely special cases of fractional Fourier domains. These fractional domains are characterized by the parameter a. Conventionally, spatial filtering has been performed in the 0th and 1st fractional domains, which are the space and frequency domains, respectively. However, in later work [1,2], it is shown that, it is possible to improve performance by filtering in fractional domains. In this paper, we used the idea of filtering in fractional Fourier domains in order to obtain the best synthesis of a desired mutual intensity distribution. More specifically, we found the optimal fractional-domain filter that transformed a given (source) mutual intensity distribution into the desired one as closely as possible (in the minimum mean-square error sense).

The ath order fractional Fourier transform $\hat{q}_a(u)$ of the function $\hat{q}(u)$ is defined for $0 < |a| < 2$ as

$$\hat{q}_a(u) \equiv \int_{-\infty}^{\infty} B_a(u,u')\,\hat{q}(u')\,\mathrm{d}u',$$

$$B_a(u,u') \equiv \frac{\exp[-\mathrm{i}(\pi\hat{\phi}/4-\phi/2)]}{|\sin\phi|^{1/2}} \exp[\mathrm{i}\pi(u^2\cot\phi - 2uu'\csc\phi + u'^2\cot\phi)], \tag{1}$$

SSDI 0030-4018(95)00768-7

where

$$\phi \equiv a\pi/2, \tag{2}$$

and $\hat{\phi} = \mathrm{sgn}(\sin\phi)$. The kernel is defined separately for $a = 0$ and $a = \pm 2$ as $B_0(u,u') \equiv \delta(u - u')$ and $B_{\pm 2}(u,u') \equiv \delta(u + u')$ respectively [3]. The definition is easily extended outside the interval $[-2,2]$ by noting that $\mathcal{F}^{4j+a}\hat{q} = \mathcal{F}^a\hat{q}$ for any integer j. Both u and u' are interpreted as dimensionless variables.

Some essential properties of the fractional Fourier transform are: (i) It is linear. (ii) The first order transform ($a = 1$) corresponds to the common Fourier transform. (iii) It is additive in index, $\mathcal{F}^{a_1}\mathcal{F}^{a_2}\hat{q} = \mathcal{F}^{a_1+a_2}\hat{q}$. (iv) The kernel for the $-a$th order transform is the conjugate of the kernel for the ath order transform: $B_a^*(u,u') = B_{-a}(u,u')$. Other properties may be found in [1,3–7,9,10].

Given the scale parameters s and s', the fraction a, and the complex amplitude distributions $q_a(\cdot)$ and $q(\cdot)$, optical implementations of the fractional Fourier transform, expressed as,

$$q_a(x) = \int_{-\infty}^{\infty} \frac{1}{s'} B_a\left(\frac{x}{s}, \frac{x'}{s'}\right) q(x')\,\mathrm{d}x', \tag{3}$$

have been presented in the literature (here, the coordinates x and x', and the scale parameters s and s' are measured in meters): In Refs. [4–6] the fractional Fourier transforming property of quadratic graded-index media is discussed, in Refs. [7,16] bulk optical systems are considered. Signal processing applications have been suggested in these references and in Refs. [1,2,8,10,13]. Further development of the role of the fractional Fourier transform in optics, as well as certain extensions and experimental results may be found in Refs. [4–6,11–15].

In Refs. [12,15,16] it is shown that there exists a fractional Fourier transform relation between the amplitude distributions of light on two spherical surfaces of given radii and separation. Unlike most other papers which deal with the implementation of the fractional transform, these papers pose the transform as a tool for analyzing and describing optical systems composed of an arbitrary sequence of thin lenses and sections of free space. The fractional transform allows one to express the evolution of the amplitude distribution of light through an optical system in terms of fractional Fourier transforms of increasing order.

In all of the references mentioned above, statistical properties of light are ignored, and full coherence is assumed. In some cases, however, this assumption cannot be justified so that the wave functions must be considered as random processes. In this paper, we deal with partially coherent light. One of the important quantities used to describe the statistical properties of light is its mutual intensity. Assuming quasi-monochromatic light, the mutual intensity can be expressed as [17,18];

$$J_q(r_1, r_2) = E\{q(r_1)\, q^*(r_2)\}, \tag{4}$$

where $E\{\cdot\}$ is the expected value operator, and $q(r)$ is the complex amplitude distribution of the optical wave.

In Ref. [19], the propagation of mutual intensity through linear quadratic-phase systems are expressed in terms of two-dimensional fractional Fourier transforms for one-dimensional systems, and four-dimensional fractional Fourier transforms for two-dimensional systems. In other words, for one dimensional systems, the expression for $J_{q_a}(x_1, x_2)$ (which is the mutual intensity of the light wave after propagating through a system characterized by Eq. (3)) is given in terms of $J_q(x_1, x_2)$ as,

$$J_{q_a}(x_1, x_2) = \int_{-\infty}^{\infty}\int_{-\infty}^{\infty} \left(\frac{1}{s'}\right)^2 B_a\left(\frac{x_1}{s}, \frac{x_1'}{s'}\right) B_{-a}\left(\frac{x_2}{s}, \frac{x_2'}{s'}\right) J_q(x_1', x_2')\,\mathrm{d}x_1'\,\mathrm{d}x_2'. \tag{5}$$

Using this result, in this paper, we dealed with the problem of synthesizing a desired mutual intensity distribution.

For simplicity, we restrict our attention to one-dimensional systems. The extension to two-dimensions is straightforward.

This paper together with [19] are not the only applications of fractional Fourier transforms to optical systems with partially coherent light. In Ref. [20] the output intensity of such systems is related to the fractional Fourier transform of the input, where the order a is related to the degree of partial coherence.

2. Definition of the problem

The mutual intensity is one of the most common ways of characterizing the spatial coherence of a wave field. Our goal in this paper is to synthesize a mutual intensity distribution $J_1(x_1, x_2)$, which is closest to a desired output mutual intensity distribution $J_1^d(x_1, x_2)$, given a source mutual intensity distribution $J_0(x_1, x_2)$. In other words, using the configuration given in Fig. 1, we want to choose the orders of the two fractional Fourier transform stages, a_1 and a_2, and the filter $H(x)$ such that the actual output $J_1(x_1, x_2)$ is as close to $J_1^d(x_1, x_2)$ as possible. More precisely, we want to minimize the following minimum mean-square error M,

$$M = \iint | J_1^d(x_1, x_2) - k J_1(x_1, x_2) |^2 \, dx_1 \, dx_2, \tag{6}$$

by choosing a_1, a_2, $H(x)$ and k appropriately. In Eq. (6) we allow for the real constant k, because we consider it sufficient to match $J_1^d(x_1, x_2)$ and $J_1(x_1, x_2)$ within a constant factor. In the expression for M, the effects of a_1, a_2 and $H(x)$ are hidden in $J_1(x_1, x_2)$ as we obtain the actual output $J_1(x_1, x_2)$ from the source mutual intensity $J_0(x_1, x_2)$ by first fractional Fourier transforming $J_0(x_1, x_2)$ with fraction a_1, then filtering by $H(x)$, and lastly fractional Fourier transforming with fraction a_2.

The expression for the propagation of the mutual intensity is given in Eq. (5). By defining new variables $u_1 \equiv x_1/s$, $u_2 \equiv x_2/s$, $u_1' \equiv x_1'/s'$ and $u_2' \equiv x_2'/s'$, and defining the scaled mutual intensities as $\hat{J}_{\hat{q}_a}(u_1, u_2) \equiv J_{q_a}(su_1, su_2)$ and $\hat{J}_{\hat{q}}(u_1', u_2') \equiv J_q(s'u_1', s'u_2')$, Eq. (5) can be rewritten as,

$$\hat{J}_{\hat{q}_a}(u_1, u_2) = \int_{-\infty}^{\infty} \int_{-\infty}^{\infty} B_a(u_1, u_1') \, B_{-a}(u_2, u_2') \, \hat{J}_{\hat{q}}(u_1', u_2') \, du_1' \, du_2', \tag{7}$$

where u_1, u_2, u_1' and u_2' are dimensionless variables. This equation can also be expressed as,

$$\hat{J}_{\hat{q}_a}(u_1, u_2) = \hat{T}_a\{\hat{J}_{\hat{q}}(u_1, u_2)\}(u_1, u_2), \tag{8}$$

where $\hat{T}_a$ is essentially the two-dimensional fractional Fourier transformation operator with fraction a (i.e., $\hat{T}_a\{\hat{J}(u_1, u_2)\} = \mathcal{F}_{u_1}^a\{\mathcal{F}_{u_2}^{-a}\{\hat{J}(u_1, u_2)\}\}$ where $\mathcal{F}_{u_i}^a\{\cdot\}$ is the fractional Fourier transform with respect to the u_ith coordinate with fraction a).

With these new definitions, the configuration given in Fig. 1 can also be expressed as the one shown in Fig. 2, and our problem boils down to the minimization of $\hat{M}$, which is defined as,

$$\hat{M} = \iint | \hat{J}_1^d(u_1, u_2) - k \hat{J}_1(u_1, u_2) |^2 \, du_1 \, du_2. \tag{9}$$

By comparing the expressions for M and $\hat{M}$, it is easy to see that $\hat{M} = M/s^2$.

As $\hat{T}_a\{\cdot\}$ is a unitary transformation, $\hat{M}$ can also be expressed on plane $1'$ (see Fig. 2) as,

$$\hat{M} = \iint | \hat{J}_{1'}^d(u_1, u_2) - k \hat{J}_{1'}(u_1, u_2) |^2 \, du_1 \, du_2, \tag{10}$$

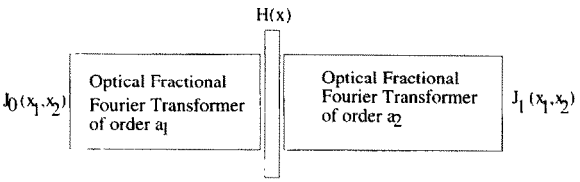

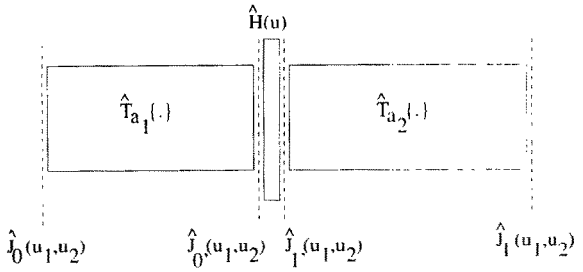

Fig. 1. A complex spatial filter $H(x)$ is inserted between two optical fractional Fourier transformer stages.

Fig. 2. Mathematical model.

where $\hat{J}_{1'}(\cdot,\cdot)$ and $\hat{J}^d_{1'}(\cdot,\cdot)$ are obtained from $\hat{J}_1(\cdot,\cdot)$ and $\hat{J}^d_1(\cdot,\cdot)$ through the operator $\hat{T}_a\{\cdot\}$ by an inverse transformation (i.e., $\hat{J}_{1'}(u_1,u_2) = \hat{T}_{-a_2}\{\hat{J}_1(u_1,u_2)\}$ and $\hat{J}^d_{1'}(u_1,u_2) = \hat{T}_{-a_2}\{\hat{J}^d_1(u_1,u_2)\}$). Referring to Fig. 2, one can see that,

$$\hat{J}_{1'}(u_1,u_2) = \hat{J}_{0'}(u_1,u_2)\,\hat{H}(u_1)\,\hat{H}^*(u_2). \tag{11}$$

By inserting Eq. (11) into Eq. (10), $\hat{M}$ expression takes the form of

$$\hat{M} = \iint |\,\hat{J}^d_{1'}(u_1,u_2) - k\hat{H}(u_1)\,\hat{H}^*(u_2)\,\hat{J}_{0'}(u_1,u_2)\,|^2\,du_1\,du_2. \tag{12}$$

As far as the optimization of $\hat{M}$ is concerned, the effect of k and $\hat{H}(.)$ can be combined by defining $\hat{H}_o(u) = \sqrt{k}\,\hat{H}(u)$. Then, $\hat{M}$ turns out to be;

$$\hat{M} = \iint |\,\hat{J}^d_{1'}(u_1,u_2) - \hat{H}_o(u_1)\,\hat{H}^*_o(u_2)\,\hat{J}_{0'}(u_1,u_2)\,|^2\,du_1\,du_2. \tag{13}$$

From this point on, we first fix a_1 and a_2 and get the optimum filter profile $\hat{H}_o(\cdot)$ which minimizes $\hat{M}$. After finding $\hat{H}_o(\cdot)$, we will calculate the corresponding $\hat{M}$ value (We will repeat this for all possible a_1 and a_2 values, and the optimum a_1 and a_2 values will then be found as the ones which correspond to the minimum $\hat{M}$ value). So, as a result of the calculus of variations method [21] applied to Eq. (13) (Appendix A), it is obtained that, for fixed a_1 and a_2, the $\hat{H}_o(\cdot)$ profiles which minimize $\hat{M}$, must also satisfy the following integral equation;

$$\int du_2\,\hat{J}^*_{0'}(u_1,u_2)\,\hat{J}^d_{1'}(u_1,u_2)\,\hat{H}_o(u_2) = \hat{H}_o(u_1)\int du_2\,|\hat{J}_{0'}(u_1,u_2)|^2\,|\hat{H}(u_2)|^2. \tag{14}$$

The above expression can also be expressed as,

$$\hat{H}_o(u_1) = \frac{\int du_2\,\hat{J}^*_{0'}(u_1,u_2)\,\hat{J}^d_{1'}(u_1,u_2)\,\hat{H}_o(u_2)}{\int du_2\,|\hat{J}_{0'}(u_1,u_2)|^2\,|\hat{H}_o(u_2)|^2}, \tag{15}$$

so that, we may obtain the $\hat{H}_o(\cdot)$ profiles in an iterative way.

It is given in Appendix B that, $\exp(i\beta)\,\hat{H}_o(u)$ is the only set of solution of Eq. (15) with arbitrary angle β. However, we don't observe the effect of angle β, because it vanishes in Eq. (11). So, without loss of generality we may take β as zero.

As a result, we first fix a_1 and a_2, and get $\hat{H}_o(u)$ profile from Eq. (15). By using this filter profile we calculate $\hat{M}$, and we do this for all a_1 and a_2 values. The optimum a_1 and a_2 values are the ones which correspond to minimum $\hat{M}$ value, and the closest $\hat{J}_1(u_1,u_2)$ profile is calculated by using the optimum a_1 and a_2 values and the corresponding $\hat{H}_o(\cdot)$ profile.

3. Synthesizing a rectangular mutual intensity profile from an incoherent source

3.1. In the previous section, the problem is defined and solved for general source and desired output mutual intensity functions. Now, let us choose specific profiles for these mutual intensities. From this point on, we consider the light source to be incoherent. As the size of the light source is assumed to extend from $-r_0$ to r_0, the mutual intensity of the source may be expressed as,

$$J_0(x_1, x_2) = \delta(x_1 - x_2)\,\mathrm{rect}\left(x_1/2r_0\right), \tag{16}$$

where the function $\mathrm{rect}(x_1/2r_0)$ is defined to be 1 when $-r_0 \leq x_1 \leq r_0$, and 0 otherwise. Using the dimensionless variables, Eq. (16) becomes,

$$\hat{J}_0(u_1, u_2) = \frac{1}{s}\,\delta(u_1 - u_2)\,\mathrm{rect}\left(\frac{u_1}{2(r_0/s)}\right). \tag{17}$$

We restrict ourselves to fractional Fourier transforming systems whose input and output scale parameters s and s' are equal. As for the desired mutual intensity, we choose to synthesize a rectangular profile, expressed as,

$$J_1^d(x_1, x_2) = \mathrm{rect}\left(\frac{|x_1 - x_2|}{2r_1}\right)\mathrm{rect}\left(\frac{x_1}{2r_2}\right)\mathrm{rect}\left(\frac{x_2}{2r_2}\right). \tag{18}$$

In other words, we want the amplitude of light at two points to be fully correlated when the distance between those points is smaller than $2r_1$, and totally uncorrelated otherwise. Moreover, we are interested in pairs of points which both lie in the region $[-r_2, r_2]$. In dimensionless variables, Eq. (18) turns out to be,

$$\hat{J}_1^d(u_1, u_2) = \mathrm{rect}\left(\frac{|u_1 - u_2|}{2(r_1/s)}\right)\mathrm{rect}\left(\frac{u_1}{2(r_2/s)}\right)\mathrm{rect}\left(\frac{u_2}{2(r_2/s)}\right). \tag{19}$$

Again s' is assumed to be equal to s. Defining the new parameters as $\hat{r}_0 \equiv r_0/s$, $\hat{r}_1 \equiv r_1/s$ and $\hat{r}_2 \equiv r_2/s$, Eqs. (17) and (19) can be rewritten as

$$\hat{J}_0(u_1, u_2) = \frac{1}{s}\,\delta(u_1 - u_2)\,\mathrm{rect}\left(\frac{u_1}{2\hat{r}_0}\right), \tag{20}$$

and

$$\hat{J}_1^d(u_1, u_2) = \mathrm{rect}\left(\frac{|u_1 - u_2|}{2\hat{r}_1}\right)\mathrm{rect}\left(\frac{u_1}{2\hat{r}_2}\right)\mathrm{rect}\left(\frac{u_2}{2\hat{r}_2}\right). \tag{21}$$

3.2. Let us express $\hat{J}_1^d(u_1, u_2)$ profile in terms of the function $\hat{J}_{1,\mathrm{scaled}}^d(u_1, u_2; \xi)$ which is defined as,

$$\hat{J}_{1,\mathrm{scaled}}^d(u_1, u_2; \xi) = \mathrm{rect}\left(\frac{|u_1 - u_2|}{2\xi}\right)\mathrm{rect}\left(\frac{u_1}{2}\right)\mathrm{rect}\left(\frac{u_2}{2}\right). \tag{22}$$

Then,

$$\hat{J}_1^d(u_1, u_2) = \hat{J}_{1,\mathrm{scaled}}^d\left(\frac{u_1}{\hat{r}_2}, \frac{u_2}{\hat{r}_2}; \xi\right), \tag{23}$$

with

$$\xi = \hat{r}_1/\hat{r}_2. \tag{24}$$

With this definition of $\hat{J}_1^d(\cdot,\cdot)$, it is given in Appendix C that, we may reduce this problem into the form of the iteration given in Eq. (15), i.e.,

$$\tilde{H}_o(u_1) = \frac{\int du_2 \,\mathrm{sinc}((u_2-u_1)\chi_n)\, I_b(u_1,u_2;\xi)\, \tilde{H}_o(u_2)}{\int du_2 \,\mathrm{sinc}^2((u_2-u_1)\chi_n)\,|\tilde{H}(u_2)|^2} \tag{25}$$

and the form of $\hat{M}$ can be expressed as,

$$\hat{M} = \hat{r}_2^2 \iint |\, I_b(u_1,u_2;\xi) - \tilde{H}_o(u_1)\, \tilde{H}_o^*(u_2)\,\mathrm{sinc}((u_2-u_1)\chi_n)\,|^2 du_1\, du_2. \tag{26}$$

In these equations,

$$\chi_n = 2\frac{\hat{r}_0}{\hat{r}_2}\csc\phi_1 \frac{\sin\phi_2}{\sin\nu} \tag{27}$$

and

$$I_b(u_1,u_2;\xi) = \int_{-\infty}^{\infty}\int_{-\infty}^{\infty} du_1'\, du_2'\, \hat{J}_{1,\mathrm{scaled}}^d(u_1',u_2';\xi)\, B_b^*(u_1',u_1)\, B_b(u_2',u_2), \tag{28}$$

with $\xi = \hat{r}_1/\hat{r}_2$ and $b = 2\nu/\pi$ where $\nu = \tan^{-1}(\tan\phi_2/\hat{r}_2^2)$. So, as a result, in Eq. (25), we were able to put the iteration in the form given in Eq. (15), and with this iteration given in Eq. (25), as far as the filter profile is concerned, we were able to sum up all the effects of the parameters, into three variables χ_n, b and ξ. In addition to this, in Eq. (26), we were able to express the form of $\hat{M}$, by using the newly defined functions and variables in Eq. (25). It is also pointed out in Appendix C that, the filter profile $\tilde{H}_o(\cdot)$, given in Eq. (25), is related to the one given in Eq. (15) through the expression,

$$\tilde{H}_o(u) = \sqrt{\frac{2\hat{r}_0|A_\nu|^2}{s\hat{r}_2^2|\sin\phi_1||A_{\phi_2}|^2}}\exp\left[i\pi\frac{u^2}{l^2}\left(\cot\phi_1+\cot\phi_2\frac{1-\hat{r}_2^4}{1+\hat{r}_2^4\cot^2\phi_2}\right)\right]\hat{H}_o\left(\frac{u}{l}\right), \tag{29}$$

where $l = \hat{r}_2|\sin\nu|/|\sin\phi_2|$.

In the Introduction part, it is given that, taking the fraction of the fractional Fourier transform in the interval $[-2,2]$ is sufficient. When the functions of interest are symmetric, as is the case here, this interval reduces to $[-1,1]$. However, in our case, we have the opportunity to reduce this interval more. When b is changed to $-b$, $I_b(\cdot,\cdot)$ becomes $I_b^*(\cdot,\cdot)$, $\tilde{H}_o(\cdot)$ becomes $\tilde{H}_o^*(\cdot)$ and $\hat{M}$ stays the same (provided that $\hat{J}_1^d(\cdot,\cdot)$ is real, as is the case here). So, as far as $\hat{M}$ is concerned, $0 \le b \le 1$ is sufficient to analyze the behavior of $\hat{M}$ under various b values.

3.3. Through the simulations, instead of $\hat{M}$, we intended to obtain the behavior of the normalized $\hat{M}$ value, which is defined as,

$$\hat{M}_{nor} = \frac{\hat{M}}{\iint |\,\hat{J}_1^d(u_1,u_2)\,|^2 du_1\, du_2}. \tag{30}$$

Using Eq. (23) and Eq. (24), we may easily see that,

$$\iint |\,\hat{J}_1^d(u_1,u_2)\,|^2 du_1\, du_2 = \hat{r}_2^2 \iint |\,\hat{J}_{1,\mathrm{scaled}}^d(u_1,u_2;\xi)\,|^2 du_1\, du_2. \tag{31}$$

We also know that,

$$I_b(u_1,u_2;\xi) = \hat{T}_{-b}\{\hat{J}_{1,\mathrm{scaled}}^d(u_1,u_2;\xi)\}. \tag{32}$$

So, as a result, using the unitary transformation property of $\hat{T}_a$, $\hat{M}_{nor}$ can be expressed as,

$$\hat{M}_{nor} = \frac{\iint | I_b(u_1,u_2;\xi) - \tilde{H}_o(u_1)\,\tilde{H}_o^*(u_2)\,\mathrm{sinc}((u_2-u_1)\chi_n)\,|^2\,\mathrm{d}u_1\,\mathrm{d}u_2}{\iint | I_b(u_1,u_2;\xi)\,|^2\,\mathrm{d}u_1\,\mathrm{d}u_2}. \tag{33}$$

It is clearly seen from Eq. (25) and Eq. (33) that, both $\tilde{H}_o(u)$ and $\hat{M}_{nor}$ are functions of only three variables b, χ_n and ξ. In order to get the behavior of $\hat{M}_{nor}$, we first fix the variables b, χ_n and ξ, and obtain the filter profile $\tilde{H}_o(\cdot)$ from Eq. (25). Then, by using this filter profile, we get $\hat{M}_{nor}$ value for these fixed b, χ_n and ξ variables.

As there are more parameters we can consider, for a specific example, we set r_2 to be $8s$ (which is equivalent to choosing $\hat{r}_2$ to be 8). Throughout the simulation program, with this $\hat{r}_2$ value (i.e., $\hat{r}_2 = 8$), we obtained $\hat{M}_{nor}$ versus a_2 plots. In order to have the simulation results to be consistent with the theory, we modified b as b' so as to have b' equal to a_2 when $\hat{r}_2 = 8$. For this reason we defined b' to be,

$$b' = 2\nu'/\pi, \tag{34}$$

where $\nu' = \tan^{-1}(64\tan\phi_2/\hat{r}_2^2)$. As is easily seen, when $\hat{r}_2$ is equal to 8, ν' becomes ϕ_2 and b' becomes a_2, which we desire to have. Using this new fraction b', $\hat{M}_{nor}$ versus b' plots with χ_n as a parameter are given in Fig. 3, Fig. 4 and Fig. 5, which correspond to $\xi = 1/2$, $\xi = 1/10$ and $\xi = 1/25$ cases, respectively.

3.4. Now, let us illustrate a numerical example. As we have more parameters we can consider, we arbitrarily set r_2 to be $8s$ (i.e., $\hat{r}_2 = 8$) and choose $\xi = 1/2$ (i.e., $r_1 = 4s$ or $\hat{r}_1 = 4$). With this choice of ξ value, we have the opportunity to look at Fig. 3. It is clearly observed in Fig. 3 that, the value of $\hat{M}_{nor}$ is minimum when $b' = 0.8$ and $\chi_n = 0.5$. Then, from this point on, we set b' to be 0.8 and χ_n to be 0.5. With $\hat{r}_2 = 8$, from Eq. (34) we have $a_2 = b' = 0.8$, and with $\hat{r}_2 = 8$ and $\hat{r}_1 = 4$ from Eq. (27) we have $\hat{r}_0/\sin\phi_1 = 2$. At this point, we arbitrarily choose $\hat{r}_0$ to be 1 (i.e., $r_0 = s$), from which we find $\sin\phi_1 = 0.5$ and $a_1 = 2\phi_1/\pi = 1/3$. So, referring to Fig. 2, with $\hat{r}_2 = 8$, $\hat{r}_1 = 4$ and $\hat{r}_0 = 1$ in order to have minimum $\hat{M}_{nor}$ value, the orders of the 1st and 2nd fractional Fourier transform stages, (i.e., a_1 and a_2), must be set to 1/3 and 0.8, respectively.

The optimum filter profile, which corresponds to these parameter values, is obtained through the iteration given in Eq. (25), and its magnitude is given in Fig. 6. By using this filter profile, we then obtained the output

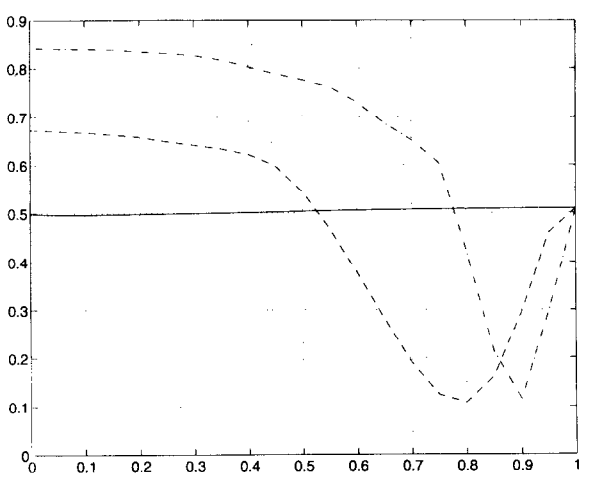

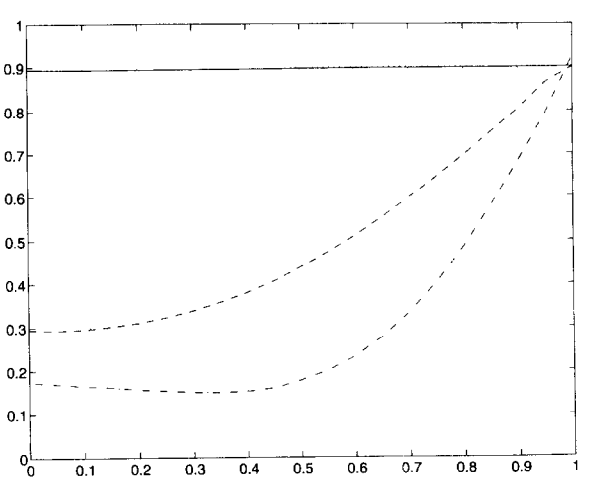

Fig. 3. M_{nor} as a function b' for $\xi = 1/2$ when $\chi_n = 0.01$ (solid line), $\chi_n = 0.50$ (dashed line), $\chi_n = 1.00$ (dash-dotted line).

Fig. 4. M_{nor} as a function b' for $\xi = 1/10$ when $\chi_n = 0.01$ (solid line), $\chi_n = 0.50$ (dashed line), $\chi_n = 1.00$ (dash-dotted line).

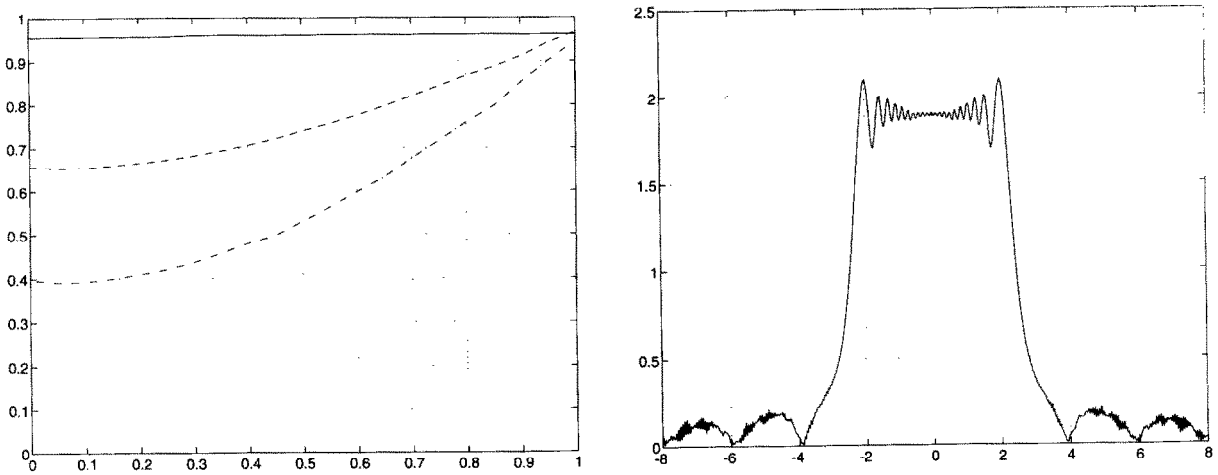

Fig. 5. M_{nor} as a function b' for $\xi = 1/25$ when $\chi_n = 0.01$ (solid line), $\chi_n = 0.50$ (dashed line), $\chi_n = 1.00$ (dash-dotted line).

Fig. 6. Magnitude of the optimum filter as a function of u when $\xi = 1/2$, $\chi_n = 0.50$ and $b' = 0.8$.

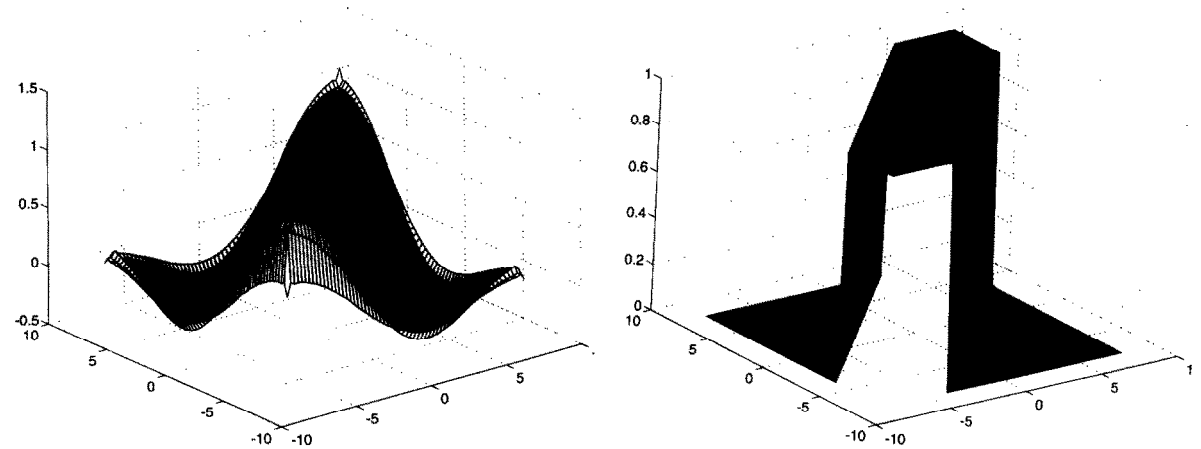

Fig. 7. Actual output mutual intensity function when $\xi = 1/2$, $\chi_n = 0.50$ and $b' = 0.8$.

Fig. 8. Desired profile for the output mutual intensity function when $\xi = 1/2$.

mutual intensity, and is shown in Fig. 7. In order to compare the output mutual intensity with the desired one, we showed the mesh plot of the desired mutual intensity in Fig. 8. For better comparison, we then obtained the profiles of both the desired mutual intensity and the output mutual intensity along $u_1 = -u_2$ axis, and we showed them on the same plot in Fig. 9.

As a result, in this example, we conclude that the closest output mutual intensity distribution to the desired profile is obtained by filtering in fractional Fourier domains, compared to filtering in conventional space and spatial frequency domains. Finally, by looking at Fig. 7, Fig. 8 and Fig. 9, we have an idea of how close the output mutual intensity is to the desired one.

In our paper, we have employed the widely used and analytically tractable minimum mean-square error criterion for purposes of illustration. However, we are not excluding the use of other error criteria. The basic

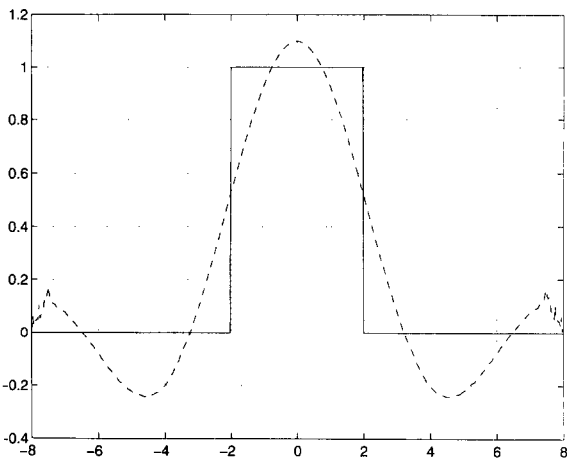

Fig. 9. Profiles of the desired mutual intensity shown in Fig. 8 and the output mutual intensity shown in Fig. 7 along $u_1 = -u_2$ axis (dashed line for the output mutual intensity, and the solid line for the desired one).

idea of our paper, that of filtering in fractional Fourier domains to synthesize desired mutual intensities, is not affected by the particular error criterion one chooses. For instance, if one considers the synthesized mutual intensity to be an inadequate approximation to the desired rectangular profile (Fig. 9), despite the fact that the normalized minimum mean-square error is reasonably small (around 0.11), it might be preferable to employ some other error criterion.

It would be possible to obtain better approximations to the desired profile by employing several consecutive fractional Fourier domain filters, rather than only one.

4. Conclusion

The mutual intensity distribution is one of the most common ways of characterizing the spatial partial coherence of a wave-field. In [19], the propagation of mutual intensity through first-order optical systems (systems involving thin spherical lenses, quadratic graded-index media, and free-space propagation in the Fresnel approximation) is expressed neatly in terms of the fractional Fourier transform. Using this fact, in this paper, we showed how to synthesize the closest (in minimum mean-square error sense) mutual intensity distribution to a desired distribution, for a given source mutual intensity profile, by using fractional Fourier domain filtering. In this paper, we also pointed out that, in some cases, closer approximations to the desired profile can be obtained by filtering in fractional Fourier domains, in comparison to filtering in the ordinary space or frequency domains.

Appendix A

Let us define a general M_g expression for a general filter profile $\hat{H}_g(\cdot)$ as

$$M_g = \iint |\hat{J}^d_{1'}(u_1, u_2) - \hat{H}_g(u_1)\, \hat{H}^*_g(u_2)\, \hat{J}_{0'}(u_1, u_2)|^2 \, \mathrm{d}u_1 \, \mathrm{d}u_2. \tag{A.1}$$

In order to follow the steps easily, let us express M_g as

$$M_g = \iint |\hat{J}_{0'}(u_1, u_2)|^2 \, |A(u_1, u_2) - \hat{H}_g(u_1)\, \hat{H}^*_g(u_2)|^2 \, du_1 \, \mathrm{d}u_2 \,, \tag{A.2}$$

where $A(u_1,u_2) = \hat{J}_1^d(u_1,u_2)/\hat{J}_{0'}(u_1,u_2)$. Let

$$\hat{H}_g(u) = \hat{H}_o(u) + \epsilon(u)\,, \tag{A.3}$$

where $\hat{H}_o(u)$ is the optimum filter profile that we are looking for, and $\epsilon(u)$ is a functional perturbation. The idea of the calculus of variations method [21] lies behind the fact that, the value of M_g cannot change considerably for $\hat{H}_g(\cdot)$ profile close to $\hat{H}_o(\cdot)$ (i.e., for $\epsilon(u)$ whose magnitude is small). Inserting Eq. (A.3) into Eq. (A.2), and assuming that the magnitude of $\epsilon(u)$ is small compared to the magnitude of $\hat{H}_o(u)$, we come up with

$$M_g = \iint |\hat{J}_{0'}(u_1,u_2)|^2\,|A(u_1,u_2) - \hat{H}_o(u_1)\,\hat{H}_o^*(u_2) - \epsilon(u_1)\,\hat{H}_o^*(u_2) - \hat{H}_o(u_1)\,\epsilon^*(u_2)|^2\,du_1\,du_2. \tag{A.4}$$

The expression for M_g can be written as,

$$M_g = \hat{M} - M_\epsilon, \tag{A.5}$$

where $\hat{M}$ is the part of M_g which is independent of the function $\epsilon(\cdot)$, i.e.,

$$\hat{M} = \iint |\hat{J}_{0'}(u_1,u_2)|^2\,|A(u_1,u_2) - \hat{H}_o(u_1)\,\hat{H}_o^*(u_2)|^2\,du_1\,du_2, \tag{A.6}$$

and M_ϵ is the remaining part of M_g (i.e., the part which depends on $\epsilon(\cdot)$). For the functions $\epsilon(\cdot)$ having small magnitude, M_ϵ can be approximated as,

$$\begin{aligned} M_\epsilon \approx{}& \iint |\hat{J}_{0'}(u_1,u_2)|^2\,\left[A(u_1,u_2) - \hat{H}_o(u_1)\hat{H}_o^*(u_2)\right]\left[\hat{H}_o^*(u_1)\epsilon(u_2) + \hat{H}_o(u_2)\epsilon^*(u_1)\right]\,du_1\,du_2 \\ &+ \iint |\hat{J}_{0'}(u_1,u_2)|^2\,\left[A^*(u_1,u_2) - \hat{H}_o^*(u_1)\hat{H}_o(u_2)\right]\left[\hat{H}_o(u_1)\epsilon^*(u_2) + \hat{H}_o^*(u_2)\epsilon(u_1)\right]\,du_1\,du_2. \end{aligned} \tag{A.7}$$

The expression for M_ϵ can be put in the form

$$\begin{aligned} M_\epsilon = {}& \int du_1\,\epsilon(u_1) \int du_2\,G(u_1,u_2) + \int du_1\,\epsilon^*(u_1) \int du_2\,G^*(u_1,u_2) \\ &+ \int du_2\,\epsilon(u_2) \int du_1\,F(u_1,u_2) + \int du_2\,\epsilon^*(u_2) \int du_1\,F^*(u_1,u_2), \end{aligned} \tag{A.8}$$

where

$$\begin{aligned} G(u_1,u_2) &= A^*(u_1,u_2)\hat{H}_o^*(u_2) - \hat{H}_o^*(u_1)|\hat{H}_o(u_2)|^2, \\ F(u_1,u_2) &= A(u_1,u_2)\hat{H}_o^*(u_1) - \hat{H}_o^*(u_2)|\hat{H}_o(u_1)|^2, \end{aligned} \tag{A.9}$$

or with change of variables

$$M_\epsilon = \int du_1\,\epsilon(u_1) \int du_2\,[G(u_1,u_2) + F(u_2,u_1)] + \int du_1\,\epsilon^*(u_1) \int du_2\,[G^*(u_1,u_2) + F^*(u_2,u_1)], \tag{A.10}$$

or

$$M_\epsilon = 2\,\mathrm{Re}\left\{\int du_1\,\epsilon(u_1) \int du_2\,[G(u_1,u_2) + F(u_2,u_1)]\right\}, \tag{A.11}$$

where $\mathrm{Re}\{\cdot\}$ operator gets the real part of the functions that it is operating on.

As a consequence of calculus of variations method, in order to have $M_\epsilon = 0$ for all $\epsilon(\cdot)$ functions, we must have

$$\int \mathrm{d}u_2 \, [G(u_1,u_2) + F(u_2,u_1)] = 0, \tag{A.12}$$

which leads to

$$\int \mathrm{d}u_2 \, \hat{J}^*_{0'}(u_1,u_2)\, \hat{J}^d_{1'}(u_1,u_2)\, \hat{H}_o(u_2) = \hat{H}_o(u_1) \int \mathrm{d}u_2 \, |\hat{J}_{0'}(u_1,u_2)|^2 \, |\hat{H}(u_2)|^2, \tag{A.13}$$

which is the integral equation that we are looking for.

Appendix B

Let us rewrite Eq. (15) once more;

$$\hat{H}_o(u_1) = \frac{\int \mathrm{d}u_2 \, \hat{J}^*_{0'}(u_1,u_2)\, \hat{J}^d_{1'}(u_1,u_2)\, \hat{H}_o(u_2)}{\int \mathrm{d}u_2 \, |\hat{J}_{0'}(u_1,u_2)|^2 \, |\hat{H}_o(u_2)|^2}. \tag{B.1}$$

Let $\alpha(u)\, H_o(u)$ is also a solution of Eq. (B.1), i.e.,

$$\alpha(u_1)\hat{H}_o(u_1) = \frac{\int \mathrm{d}u_2 \, \hat{J}^*_{0'}(u_1,u_2)\, \hat{J}^d_{1'}(u_1,u_2)\, \alpha(u_2)\hat{H}_o(u_2)}{\int \mathrm{d}u_2 \, |\hat{J}_{0'}(u_1,u_2)|^2 \, |\alpha(u_2)\hat{H}_o(u_2)|^2}. \tag{B.2}$$

$\alpha(u) = 0$ is the ill-case of the problem, so it is omitted. By defining new functions as $\mathcal{J}_{0'}(u_1,u_2) = \hat{J}_{0'}(u_1,u_2)\alpha^*(u_2) / \alpha^*(u_1)$ and $\mathcal{J}^d_{1'}(u_1,u_2) = \hat{J}^d_{1'}(u_1,u_2) / |\alpha(u_1)|^2$, Eq. (B.2) can be rewritten as,

$$\hat{H}_o(u_1) = \frac{\int \mathrm{d}u_2 \, \mathcal{J}^*_{0'}(u_1,u_2)\, \mathcal{J}^d_{1'}(u_1,u_2)\, \hat{H}_o(u_2)}{\int \mathrm{d}u_2 \, |\mathcal{J}_{0'}(u_1,u_2)|^2 \, |\hat{H}_o(u_2)|^2}, \tag{B.3}$$

which is in the form of Eq. (B.1). As we are all dealing with mutual intensity profiles, $\mathcal{J}_{0'}(u_1,u_2)$ function, which satisfies Eq. (B.3) must also be conjugate symmetric. Using the definition of $\mathcal{J}_{0'}(u_1,u_2)$, and the conjugate symmetric property of it (i.e., $\mathcal{J}_{0'}(u_1,u_2) = \mathcal{J}^*_{0'}(u_2,u_1)$, $\forall u_1,u_2$), one ends up with the conclusion that, $|\alpha(u_2)|^2 = |\alpha(u_1)|^2$, $\forall u_1,u_2$, which implies that $\alpha(u)$ must be a complex constant (i.e., $\alpha(u) = a$). So,

$$a\,\hat{H}_o(u_1) = \frac{\int \mathrm{d}u_2 \, \hat{J}^*_{0'}(u_1,u_2)\, \hat{J}^d_{1'}(u_1,u_2)\, a\,\hat{H}_o(u_2)}{\int \mathrm{d}u_2 \, |\hat{J}_{0'}(u_1,u_2)|^2 \, |a|^2 \, |\hat{H}_o(u_2)|^2}. \tag{B.4}$$

Realizing that both Eq. (B.1) and Eq. (B.4) is satisfied, one can conclude that $|a| = 1$.

As a result, $\exp(\mathrm{i}\beta)\, \hat{H}_o(u)$ is the only set of solution of the iteration with arbitrary angle β.

Appendix C

Let us repeat the expression of $\hat{J}^d_{1'}(\cdot,\cdot)$ here once more i.e.,

$$\hat{J}^d_{1'}(u_1,u_2) = \hat{T}_{-a_2}\{\hat{J}^d_1(u_1,u_2)\} = \int_{-\infty}^{\infty}\int_{-\infty}^{\infty} \mathrm{d}u'_1 \, \mathrm{d}u'_2 \, \hat{J}^d_1(u'_1,u'_2)\, B^*_{a_2}(u'_1,u_1)\, B_{a_2}(u'_2,u_2). \tag{C.1}$$

We see from Eq. (23) that,

$$\hat{J}_1^d(u_1,u_2) = \hat{J}_{1,\text{scaled}}^d\left(\frac{u_1}{\hat{r}_2},\frac{u_2}{\hat{r}_2};\xi\right), \tag{C.2}$$

where $\xi = \hat{r}_1/\hat{r}_2$. Using the result of the theorem given in Appendix D, after some algebra, $\hat{J}_{1'}^d(u_1,u_2)$ can be expressed as,

$$\hat{J}_{1'}^d(u_1,u_2) = \frac{\hat{r}_2^2|A_{\phi_2}|^2}{|A_\nu|^2}\exp\left(i\pi(u_2^2-u_1^2)\cot\phi_2\frac{1-\hat{r}_2^4}{1+\hat{r}_2^4\cot^2\phi_2}\right) I_b\left(\frac{u_1\hat{r}_2\csc\phi_2}{\csc\nu},\frac{u_2\hat{r}_2\csc\phi_2}{\csc\nu};\xi\right), \tag{C.3}$$

where

$$I_b(u_1,u_2;\xi) = \int_{-\infty}^{\infty}\int_{-\infty}^{\infty} du_1'\,du_2'\,\hat{J}_{1,\text{scaled}}^d(u_1',u_2';\xi)\,B_b^*(u_1',u_1)\,B_b(u_2',u_2), \tag{C.4}$$

with $\xi = \hat{r}_1/\hat{r}_2$, $b = 2\nu/\pi$ and $\nu = \tan^{-1}(\tan\phi_2/\hat{r}_2^2)$.

Now, let's repeat the expression of $\hat{J}_{0'}(\cdot,\cdot)$ i.e.,

$$\hat{J}_{0'}(u_1,u_2) = \hat{T}_{a_1}\{\hat{J}_0(u_1,u_2)\} = \int_{-\infty}^{\infty}\int_{-\infty}^{\infty} du_1'\,du_2'\,\hat{J}_0(u_1',u_2')\,B_{a_1}(u_1',u_1)\,B_{a_1}^*(u_2',u_2). \tag{C.5}$$

Using the expression for $\hat{J}_0(\cdot,\cdot)$ given in Eq. (17), $\hat{J}_{0'}(\cdot,\cdot)$ can be expressed as,

$$\hat{J}_{0'}^s(u_1,u_2) = \frac{2\hat{r}_0}{s|\sin\phi_1|}\exp[i\pi(u_1^2-u_2^2)\cot\phi_1]\,\text{sinc}[(u_2-u_1)2\hat{r}_0\csc\phi_1], \tag{C.6}$$

where $\text{sinc}(u) = \sin(\pi u)/(\pi u)$.

Using the expressions given through Eq. (C.3) and Eq. (C.6), the iteration, which is given in Eq. (15), can be expressed as;

$$\ddot{H}_o(u_1) = \frac{\int du_2\,\text{sinc}[(u_2-u_1)2\hat{r}_0\csc\phi_1]\,I_b(u_1\hat{r}_2\csc\phi_2/\csc\nu,\,u_2\hat{r}_2\csc\phi_2/\csc\nu;\xi)\,\ddot{H}_o(u_2)}{\int du_2\,\text{sinc}^2[(u_2-u_1)2\hat{r}_0\csc\phi_1]\,|\ddot{H}(u_2)|^2}, \tag{C.7}$$

where

$$\ddot{H}_o(u_1) = \sqrt{\frac{2\hat{r}_0|A_\nu|^2}{s|\sin\phi_1|\hat{r}_2^2|A_{\phi_2}|^2}}\exp\left[i\pi u_1^2\left(\cot\phi_1+\cot\phi_2\frac{1-\hat{r}_2^4}{1+\hat{r}_2^4\cot^2\phi_2}\right)\right]\hat{H}_o(u_1). \tag{C.8}$$

Now, let's analyze what happens to $\hat{M}$. When the expressions for $\hat{J}_{1'}^d(\cdot,\cdot)$ and $\hat{J}_{0'}(\cdot,\cdot)$, which are given in Eq. (C.3) and Eq. (C.6), are used in Eq. (13), the expression for $\hat{M}$, after straightforward but lengthy algebra, comes out to be,

$$\hat{M} = \hat{r}_2^2\iint\left|I_b(u_1,u_2;\xi) - \ddot{H}_o\left(\frac{u_1}{l}\right)\ddot{H}_o^*\left(\frac{u_2}{l}\right)\text{sinc}\left((u_2-u_1)\frac{2\hat{r}_0}{l\sin\phi_1}\right)\right|^2 du_1\,du_2, \tag{C.9}$$

where $l = \hat{r}_2|\sin\nu|/|\sin\phi_2|$. If we look at Eq. (C.7), we see that,

$$\ddot{H}_o\left(\frac{u_1}{l}\right) = \frac{\int du_2\,\text{sinc}\left((u_2-u_1)\,2\hat{r}_0/l\sin\phi_1\right)\,I_b(u_1,u_2;\xi)\,\ddot{H}_o\left(u_2/l\right)}{\int du_2\,\text{sinc}^2\left((u_2-u_1)\,2\hat{r}_0/l\sin\phi_1\right)\,|\ddot{H}\left(u_2/l\right)|^2}. \tag{C.10}$$

In other words, $\ddot{H}_o(u_1/l)$ is the filter profile obtained, when $\operatorname{sinc}\left((u_2-u_1)\,2\hat{r}_0/l\sin\phi_1\right)$ and $I_b(u_1,u_2;\xi)$ is used through the iteration given in Eq. (15). So, when $\tilde{H}_o(u)$ is chosen as $\tilde{H}_o(u)=\ddot{H}_o(u/l)$, the expression for $\hat{M}$ turns out to be

$$\hat{M}=\hat{r}_2^2\iint\left|I_b(u_1,u_2;\xi)-\tilde{H}_o(u_1)\,\tilde{H}_o^*(u_2)\operatorname{sinc}\left((u_2-u_1)\frac{2\hat{r}_0}{l\sin\phi_1}\right)\right|^2\mathrm{d}u_1\,\mathrm{d}u_2\,. \tag{C.11}$$

As a result, with the given $\hat{J}_{1'}^d(\cdot,\cdot)$ and $\hat{J}_{0'}(\cdot,\cdot)$ profiles,

$$\hat{M}=\hat{r}_2^2\iint\left|I_b(u_1,u_2;\xi)-\tilde{H}_o(u_1)\,\tilde{H}_o^*(u_2)\operatorname{sinc}\left((u_2-u_1)\chi_n\right)\right|^2\mathrm{d}u_1\,\mathrm{d}u_2 \tag{C.12}$$

and

$$\tilde{H}_o(u_1)=\frac{\int\mathrm{d}u_2\operatorname{sinc}((u_2-u_1)\chi_n)\,I_b(u_1,u_2;\xi)\,\tilde{H}_o(u_2)}{\int\mathrm{d}u_2\operatorname{sinc}^2((u_2-u_1)\chi_n)\,|\tilde{H}(u_2)|^2}\,, \tag{C.13}$$

where

$$\chi_n=2\frac{\hat{r}_0}{\hat{r}_2}\csc\phi_1\frac{\sin\phi_2}{\sin\nu}\,, \tag{C.14}$$

and

$$I_b(u_1,u_2;\xi)=\int_{-\infty}^{\infty}\int_{-\infty}^{\infty}\mathrm{d}u_1'\,\mathrm{d}u_2'\,\hat{J}_{1,\mathrm{scaled}}^d(u_1',u_2';\xi)\,B_b^*(u_1',u_1)\,B_b(u_2',u_2)\,, \tag{C.15}$$

with $\xi=\hat{r}_1/\hat{r}_2$ and $b=2\nu/\pi$ where $\nu=\tan^{-1}(\tan\phi_2/\hat{r}_2^2)$.

Finally, $\tilde{H}_o(u)$ is related to $\hat{H}_o(u)$ by

$$\tilde{H}_o(u)=\sqrt{\frac{2\hat{r}_0|A_\nu|^2}{s\hat{r}_2^2|\sin\phi_1||A_{\phi_2}|^2}}\exp\left[\mathrm{i}\pi\frac{u^2}{l^2}\left(\cot\phi_1+\cot\phi_2\frac{1-\hat{r}_2^4}{1+\hat{r}_2^4\cot^2\phi_2}\right)\right]\hat{H}_o\left(\frac{u}{l}\right), \tag{C.16}$$

where $l=\hat{r}_2|\sin\nu|/|\sin\phi_2|$.

Appendix D

Theorem: $(\mathcal{F}^a\hat{f}_s)(u)$ of the function $\hat{f}_s(u)=\hat{f}(ku)$ can be expressed in terms of $(\mathcal{F}^a\hat{f})(u)$ as;

$$(\mathcal{F}^a\hat{f}_s)(u)=\frac{A_\phi}{kA_\nu}\exp\left(\mathrm{i}\pi u^2\cot\phi\frac{k^4-1}{k^4+\cot^2\phi}\right)(\mathcal{F}^b\hat{f})\left(u\frac{\sin\nu}{k\sin\phi}\right), \tag{D.1}$$

where $\nu=\tan^{-1}(k^2\tan\phi)$ (ν is assumed to be in the range $-\pi\le\nu<\pi$), $b=2\nu/\pi$ and k is any real number different from zero.

Proof:

Using the conventional definition of the fractional Fourier transform, $(\mathcal{F}^a\hat{f}_s)(u)$ can be expressed as,

$$(\mathcal{F}^a\hat{f}_s)(u)=\int_{-\infty}^{\infty}A_\phi\exp[\mathrm{i}\pi(u^2\cot\phi-2uu'\csc\phi+u'^2\cot\phi)]\,f(ku')\,\mathrm{d}u'\,. \tag{D.2}$$

If we let $v' = ku'$, the above expression comes out to be

$$(\mathcal{F}^a \hat{f}_s)(u) = \frac{1}{|k|} \int_{-\infty}^{\infty} A_\phi \exp\left[i\pi \left(u^2 \cot\phi - 2u \frac{v'}{k} \csc\phi + \frac{v'^2}{k^2} \cot\phi \right) \right] f(v')\, dv' . \tag{D.3}$$

Letting $\cot\nu = \cot\phi / k^2$ and $v = u \csc\phi / k \csc\nu$, after some algebra we end up with the result given in the theorem, i.e.,

$$(\mathcal{F}^a \hat{f}_s)(u) = \frac{A_\phi}{kA_\nu} \exp\left(i\pi u^2 \cot\phi \frac{k^4 - 1}{k^4 + \cot^2\phi} \right) (\mathcal{F}^b \hat{f}) \left(u \frac{\sin\nu}{k \sin\phi} \right) . \tag{D.4}$$

References

[1] H.M. Ozaktas, B. Barshan, D. Mendlovic, and L. Onural, J. Opt. Soc. Am. A 11 (1994) 547.
[2] A. Kutay, H.M. Ozaktas, L. Onural, O. Arikan, Proc. of IEEE International Conference on Acoustics, Speech, and Signal Processing, 1995.
[3] A.C. McBride and F.H. Kerr, IMA J. Appl. Mathematics 39 (1987) 159.
[4] H.M. Ozaktas and D. Mendlovic, Optics Comm. 101 (1993) 163.
[5] D. Mendlovic and H.M. Ozaktas, J. Opt. Soc. Am. A 10 (1993) 1875.
[6] H.M. Ozaktas and D. Mendlovic, J. Opt. Soc. Am. A 10 (1993) 2522.
[7] A.W. Lohmann, J. Opt. Soc. Am. A 10 (1993) 2181.
[8] H.M. Ozaktas, O. Arikan, A. Kutay, G. Bozdağı, IEEE Trans. on Signal Processing, submitted.
[9] A.W. Lohmann and B.H. Soffer, J. Opt. Soc. Am. A 11 (1994) 1798.
[10] L.B. Almeida, IEEE Trans. on Signal Processing 42 (1994) 3084.
[11] P. Pellat-Finet, Optics Lett. 19 (1994) 1388.
[12] P. Pellat-Finet and G. Bonnet, Optics Comm. 111 (1994) 141.
[13] L.M. Bernardo and O.D.D. Soares, Optics Comm. 110 (1994) 517.
[14] L.M. Bernardo and O.D.D. Soares, J. Opt. Soc. Am. A, to appear.
[15] H.M. Ozaktas and D. Mendlovic, Optics Lett., submitted.
[16] H.M. Ozaktas and D. Mendlovic, J. Opt. Soc. Am. A, to appear.
[17] B.E.A. Saleh, M.C. Teich, Fundamentals of Photonics (Wiley, New York, 1991) p. 355.
[18] J.W. Goodman, Statistical Optics (Wiley, New York, 1985) p. 180.
[19] M. Fatih Erden, H.M. Ozaktas and D. Mendlovic, J. Opt. Soc. Am. A, to appear.
[20] Z. Zalevsky, D. Mendlovic, E. Marom, Y. Bitran and H.M. Ozaktas, J. Opt. Soc. Am. A, submitted.
[21] D.E. Kirk, Optimal Control Theory (Prentice-Hall, New York, 1970).